JVSTB Journal of Vacuum Science & Technology B

Behavior of a new ordered structural dopant source in InAs/(001) GaP heterostructures

V. Gopal, E.-H. Chen, E. P. Kvam, and J. M. Woodall

Citation: Journal of Vacuum Science & Technology B **17**, 1767 (1999); doi: 10.1116/1.590823
View online: http://dx.doi.org/10.1116/1.590823
View Table of Contents: http://scitation.aip.org/content/avs/journal/jvstb/17/4?ver=pdfcov
Published by the AVS: Science & Technology of Materials, Interfaces, and Processing

Behavior of a new ordered structural dopant source in InAs/(001) GaP heterostructures

V. Gopal,[a] E.-H. Chen, E. P. Kvam, and J. M. Woodall
Purdue University, W. Lafayette, Indiana 47907

(Received 19 January 1999; accepted 17 May 1999)

We report the characteristics of molecular-beam epitaxy grown InAs on highly lattice mismatched (001) GaP substrates. Strain relaxation in this system occurs at low thickness by the generation of a periodic two-dimensional square grid network of 90° misfit dislocations at the heterointerface. The very high interface dislocation density ($\sim 10^{13}$ intersections/cm^2) exerts a unique influence on the electronic properties of the system. An extended defect structure at the intersection of 90° misfit dislocations is proposed to act as an ordered structural donor source. Hall effect measurements indicate that this source is fully ionized with a constant sheet carrier concentration of 10^{13} cm^{-2}, irrespective of the InAs layer thickness, and exhibits no freeze out at low temperatures. We have also demonstrated that the electron mobility increases significantly with InAs layer thickness, reaching values in excess of 10 000 cm^2/V s in nominally undoped layers. The high threading dislocation density ($\sim 10^{10}$ cm^{-2}) in the InAs epilayers does not appear to have a deleterious effect on the transport properties of majority carrier electrons. [S0734-211X(99)06904-8]

I. INTRODUCTION

Advances in the molecular-beam epitaxial (MBE) growth of compound semiconductors have resulted in the growth of a wide variety of III–V compounds and their alloys on the commercially available (001) oriented substrates such as GaAs, InP, and GaP. The growth only of lattice-matched epilayers, such as $Al_xGa_{1-x}As$ on GaAs, places a limit on the band gap range available for device design. While lattice-mismatched epitaxy removes this constraint, the consequent mismatch strain is accommodated by the generation of misfit dislocations (MD) if a critical layer thickness is exceeded. Much effort has been devoted to understanding the mechanisms of MD generation and minimizing their propagation into the epilayer as threading dislocations (TD).[1,2] However, when the lattice mismatch is high (>7%), MDs and TDs can no longer be avoided. In order to design devices using highly lattice-mismatched systems the electronic behavior of the dislocations must be understood.

Highly lattice-mismatched systems are well suited for a study of MDs for two reasons. First, the interface dislocation population is very high, so that the interface electronic properties tend to be dominated by those of the dislocations. Second, unlike in the case of lower mismatch where an irregularly spaced network of interfacial dislocations results, high mismatches favor the generation of a regular periodic network of 90° misfit dislocations oriented in the [110] and the [1$\bar{1}$0] crystallographic directions. The periodicity imposed by such a ''superlattice'' dislocation microstructure results in interesting electronic behavior.

In the present study, we have investigated the direct growth of InAs on (001) GaP substrates. The lattice mismatch is 11%, the largest among all the III-arsenides and the III-phosphides. The difference in band gap is also large: InAs–0.36 eV, GaP–2.25 eV. $Al_xIn_{1-x}As$ layers with $x = 0.1$ and 0.2 grown on GaP, which have a higher band gap than InAs but not very significantly different lattice parameters, have also been studied.

II. EXPERIMENT

InAs/GaP heterostructures were grown by solid source MBE using a Varian Gen-II system. Commercially obtained GaP substrates were heated to 710 °C for oxide desorption under a P_2 overpressure. A 20 period superlattice consisting of 5 nm alternating layers of GaP/AlGaP was grown to prevent the outdiffusion of impurities from the substrate. This was followed by the growth of a 200 nm buffer layer of undoped GaP at 660 °C. The growth of phosphides was achieved by using a valved phosphorous cracker.[3,4] Reflection high-energy electron diffraction was used to monitor surface morphology, growth rate, and surface V–III incorporation ratio.

The substrate temperature was lowered to 350 °C for the growth of an undoped InAs epilayer. At higher temperatures (450–500 °C), an interfacial reaction between the InAs and GaP was reported to occur. The first few monolayers were grown under low V/III ratios to promote a smoother interface.[3] Finally, a 5 nm capping layer of undoped $Al_{0.2}In_{0.8}As$ was grown above the InAs layer to suppress carrier generation due to surface Fermi level pinning. Samples with varying thickness of InAs ranging from 3 nm to 2 μm were grown in this manner. Figure 1 is a schematic of the multilayer structure. The growth of $Al_xIn_{1-x}As$ on GaP was carried out similarly and these layers were capped by growing the final 5 monolayers with a higher Al fraction.

Transmission electron microscopy (TEM) was employed for defect microstructure investigations. Cross-sectional samples were prepared and examined in a JEOL 2000 FX microscope with an accelerating voltage of 200 kV to obtain

[a]Electronic mail: gopal@ecn.purdue.edu

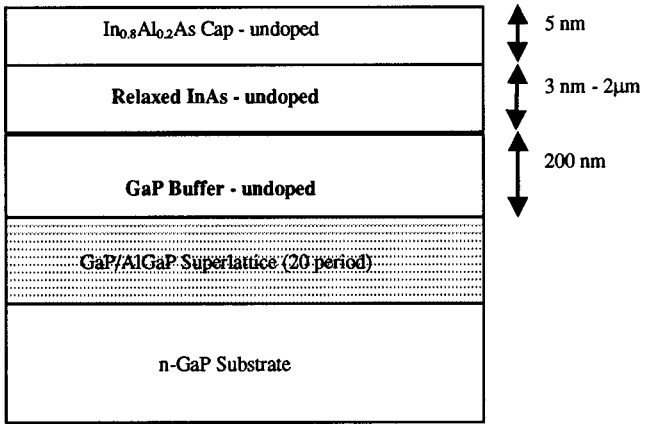

FIG. 1. Schematic of the multilayer structure grown by MBE.

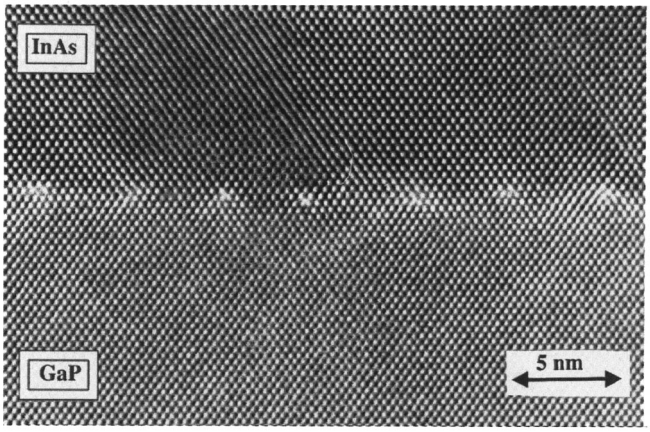

FIG. 2. HREM micrograph of InAs/GaP heterostructure. MDs appear as bright spots.

high resolution TEM (HREM) images of the heterointerface. Plan view samples were examined in a JEOL 200 CX microscope. 200 and 220 weak beam dark field images were obtained to study the threading dislocation microstructure in InAs epilayers.

Electrical properties were characterized using the Hall effect technique and electrochemical capacitance–voltage (ECV) depth carrier concentration profiling. Systematic Hall effect measurements were performed at both room temperature (300 K) and liquid N_2 temperature using the van der Pauw technique on InAs/GaP and $Al_xIn_{1-x}As$/GaP heterostructure samples. Variable temperature Hall effect data between 5 and 310 K were obtained for select samples. The majority carrier type, density, and mobility were determined from the data in the standard manner.

III. RESULTS AND DISCUSSION

A. Microstructure evolution

Strain relaxation during epitaxial growth occurs by the generation of a network of MDs in the interfacial (001) plane. Low mismatch strains (<2%) are accommodated predominantly by the glissile 60° interfacial dislocation segments formed during the glide of epithreading dislocations. Dislocation nucleation sources have been proposed to be active at the free surface of the growing film.[5] The resulting network consists of irregularly spaced long MD segments. At higher mismatches (2%–4%), the formation of short sessile 90° MD segments were observed by Kvam, Maher, and Humphreys,[6] who proposed a dislocation reaction between two complementary 60° dislocations to yield a 90° MD, e.g.,

$$\tfrac{1}{2}[0\bar{1}\bar{1}] \text{ on } (\bar{1}\bar{1}1)+\tfrac{1}{2}[\bar{1}0\bar{1}] \text{ on } (1\bar{1}\bar{1})=\tfrac{1}{2}[\bar{1}\bar{1}0] \text{ on } (001). \quad (1)$$

For very high mismatch (>7%), the MD microstructure consists of a regular, periodic network of 90° misfit dislocations. Direct introduction of sessile 90° dislocations at the edge of Ge islands growing on (001) Si (4% mismatch) has been reported by LeGoues *et al.*[7] Strain relaxation in the InAs/GaP system is expected to yield such a regular periodic MD network.

However, our HREM images provide evidence that strain relaxation in this system occurs through both direct introduction and by the glide of 60° dislocations, with the former being the dominant mechanism. Chang, Chin, and Woodall[3] reported that 2.5 nm InAs films grown on GaP were 85% strain relaxed with a dislocation spacing of 4.1 ± 0.1 nm. They did not observe any 60° MDs in their HREM images and proposed that the 90° dislocations were directly incorporated into the growing InAs layer. As the layer thickness is increased the energy required for direct introduction of MDs becomes very high, and further strain relaxation must occur by the glide and reaction of 60° MDs to form 90° dislocation segments. Evidence for this mechanism is seen in Fig. 2, which is a HREM micrograph from a 15 nm InAs sample. A closely spaced pair of 60° dislocations is observed and a Burgers circuit around this pair yields a closure gap corresponding to that of a 90° edge dislocation. Table I shows the degree of strain relaxation for InAs layers of varying thickness grown on GaP. At about 30 nm strain relaxation is complete, with a mean dislocation spacing of ~3.85 nm.

Figure 3 is a 220 dark field micrograph of a 1 μm InAs epilayer. Threading dislocations are seen at a density of $\sim 10^{10}$ cm^{-2}. While this is a high density, it is comparable to those in ~2% mismatched SiGe layers grown on Si, where the MD population is significantly less dense. A simple calculation, assuming that each MD segment is associated with two TDs at its ends, yields an average MD segment length of 10 μm. This is far in excess of the size of InAs islands (~10–100 nm) during the initial stages of growth, and implies that a single MD propagates through several islands as

TABLE I. Degree of strain relaxation of InAs epilayers of differing thickness grown on GaP.

InAs layer thickness (nm)	Mean dislocation spacing (nm)	% strain relaxed
3.0	4.19	91
15	3.95	97.5
30	3.85	100

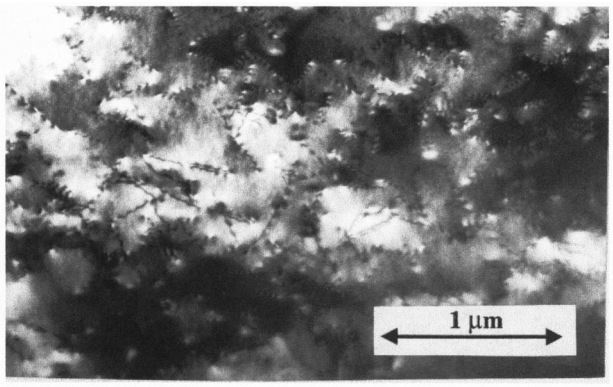

FIG. 3. Plan view TEM micrograph showing dense TD network in the InAs epilayer.

the islands coalesce without the dislocation threading into the epilayer. In summary, the dislocation microstructure consists of a regularly spaced network of (predominantly) 90° MDs with a few (<5%) closely spaced pairs of 60° dislocations. Isolated 60° MD segments have not been identified in HREM micrographs, but their occurrence cannot be ruled out.

The atomic level core structures of 90° MDs in zinc blende crystal structures have a sevenfold-fivefold ring structure, as shown in Fig. 4. Such dislocations do not have dangling bonds associated with them. We believe this to be the dominant MD core structure in the InAs/GaP system. On the other hand, 60° MDs can have dangling bonds at their cores. 90° MDs can also take on an eightfold-sixfold ring configuration with two dangling bonds per Burgers vector length at their core. The fraction of 90° MDs with this core structure is not known in InAs/GaP, but we believe it to be small.

Mostoller, Chisholm, and Kaplan proposed the occurrence of an 18 atom point defect structure—the ''dreidl''—at the

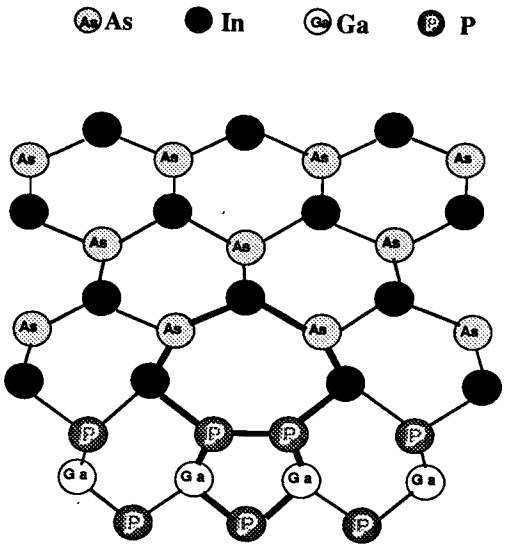

FIG. 4. Sevenfold-fivefold ring structure of a 90° MD.

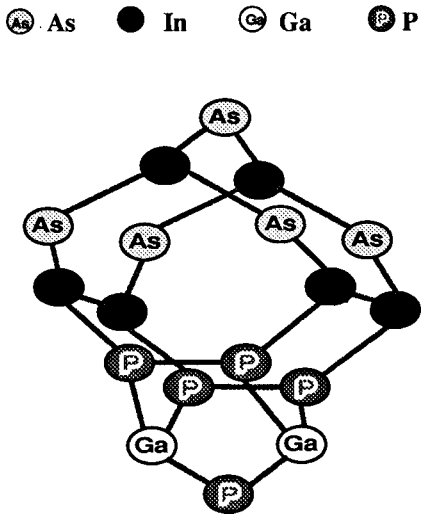

FIG. 5. 18 atom dreidl. Note the occurrence of Group III and Group V dipoles.

intersection of 90° MDs in Ge/(001) Si.[8] A similar defect structure would exist in the InAs/GaP system and is shown schematically in Fig. 5. Of particular interest is the occurrence of both III–III and V–V dipoles in each dreidl, which could contribute to the electrical activity of these defects.

B. Electronic behavior

Even though all the samples were nominally undoped, the sign of the Hall coefficient indicated *n*-type conductivity. This may be due to the large hole to electron effective mass ratio for InAs. Hence, donor-like defect levels will be shallower than acceptor levels.[4] Table II displays the sheet carrier concentration (N_s) and Hall mobility (μ) for the InAs/GaP samples tested at 300 and 77 K.[4,9] The sheet carrier concentration is very high— 10^{13} cm^{-2}—for the thin layer samples (Sample Nos. 1 through 5), and does not vary with epilayer thickness. This implies a high density of carriers localized at either the heterointerface or at the free surface. Since the InAs is capped off by an $Al_{0.2}In_{0.8}As$ layer, surface generation and accumulation was prevented. ECV profiling confirms that the carriers are localized at the InAs/GaP interface. Figure 6 is a semilog plot of carrier concentration versus depth for an ~1 μm InAs layer grown on GaP. Carrier accumulation is clearly seen on the low bandgap (InAs) side of the heterojunction.

There is also no freeze out, even at 5 K. Variable temperature Hall measurements were performed on Sample No. 4 as a representative of the thin layer samples, and the plot of N_s versus temperature is shown in Fig. 7. The sheet carrier concentration remains constant with temperature down to the lowest temperature, 5 K. This strongly indicates that the states contributing to the interfacial carriers lie above the conduction band edge of InAs and are degenerate. There are several possible sources for these carriers:

TABLE II. Sheet carrier density and electron mobility data for InAs/GaP heterostructures at 300 and 77 K.

Sample No.	InAs layer thickness (nm)	300 K		77 K	
		Sheet density ($\times 10^{13}$ cm^{-2})	Hall mobility (cm^2/V s)	Sheet density ($\times 10^{13}$ cm^{-2})	Hall mobility (cm^2/V s)
1	5	1.2	40	1.2	25
2	10	1.1	500	1.0	360
3	15	0.75	340	0.75	310
4[a]	20	1.0	460	0.8	430
5	30	1.0	800	0.9	730
6	250	1.0	4000	1.0	3 780
7[a]	500	1.2	5310	1.1	5 390
8	1000	1.5	7620	1.3	8 120
9	2000	2.0	9920	1.6	10 900

[a]5 K data.

(1) Atomic sites along 90° MDs: There are a total of 10^{14} sites along 90° MD lines per cm^2, but the measured sheet carrier concentration is an order of magnitude lower. Since the energy states responsible for these carriers do not display freeze out, it is unlikely that a fractional ionization event occurs.
(2) Atomic sites along 60° MDs: A small fraction (<5%), of closely spaced pairs of 60° MDs have been observed. Such dislocations can have dangling bonds at their cores that would be expected to display electrical activity. However, the sites along these dislocations would not be sufficient in number to account for 10^{13} carriers per cm^2.
(3) TDs: While TDs may be electrically active, they are not sufficiently dense ($\sim 10^{10}$ cm^{-2}) to account for the carriers in the thin layer samples. More importantly, TD contribution would result in a thickness dependence of N_s, which is not observed.
(4) Intrinsic band bending: InAs and GaP have large conduction and valence band offsets. However, calculations carried out using the band structure simulator ADEPT show that the intrinsic band bending would result in the Fermi level being pinned midgap in the InAs at the interface and, consequently, low carrier accumulation. A high density (10^{13} cm^{-2}) sheet of electronic charge at the interface requires the Fermi level to be pinned 0.2 eV above the conduction band edge of InAs at the interface.[9] This could be accomplished by a defect related donor state.
(5) 90° MD intersection sites: The dreidl structure (Fig. 5) might occur at the intersection of 1/2⟨110⟩ 90° MDs at the InAs/GaP interface, forming a square lattice with a periodicity of ~4 nm. These would appear with a density of $\sim 10^{13}$ cm^{-2}, a numeric match with the N_s values of Table II. Thus, the MD intersection sites may act as an array of ordered structural dopants. As mentioned previously, this structure in III–V compounds would contain strong internal dipoles, which may be the carrier generation source.

The carriers thus generated are confined to a two-dimensional electron gas near the interface and are scattered strongly by the dense MD network, as evidenced by the low mobility values in Table II. As the temperature is decreased,

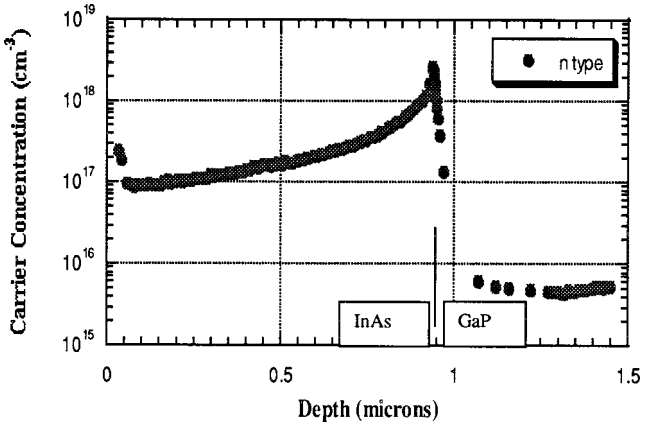

FIG. 6. ECV profile of InAs/GaP heterostructure showing carrier accumulation at the interface.

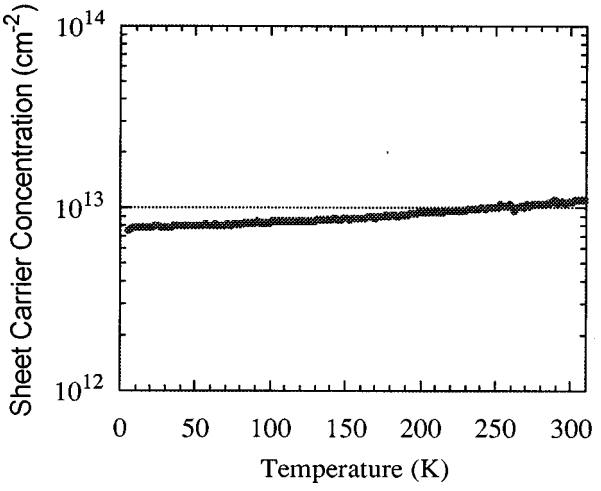

FIG. 7. Variation of sheet carrier concentration, N_s, with temperature. Note the absence of freeze out down to 5 K.

TABLE III. Comparative values of sheet carrier concentration and mobility for InAs and $Al_xIn_{1-x}As$ samples grown on GaP.

Epilayer thickness (nm)	Sample	300 K		77 K		5 K	
		N_s (cm^{-2})	μ ($cm^2/V\,s$)	N_s (cm^{-2})	μ ($cm^2/V\,s$)	N_s (cm^{-2})	μ ($cm^2/V\,s$)
20	InAs	1.0×10^{13}	460	0.8×10^{13}	430	0.75×10^{13}	470
20	$Al_{0.1}In_{0.9}As$	0.47×10^{13}	190	0.55×10^{13}	123	0.55×10^{13}	85
20	$Al_{0.2}In_{0.8}As$	5.0×10^{11}	380	7.4×10^{10}	290	...	...

the confinement would be stronger, i.e., the mobility would decrease with decreasing temperature which is consistent with our observations.[9]

Table III is a comparison of the sheet carrier concentration and mobility data for 20-nm-thick samples of InAs and $Al_xIn_{1-x}As$ ($x=0.1,0.2$). The addition of Al increases the band gap very significantly while retaining a large lattice mismatch with GaP, so the MD microstructure is expected to remain smaller. It is clear that the electronic properties differ considerably. N_s decreases with increasing Al content and carriers freeze out even at 77 K for the $Al_{0.2}In_{0.8}As$ sample. The energy states contributing to interfacial carriers are nondegenerate in this case and must lie within the band gap. Both the conduction band and the valence band offsets decrease upon addition of Al, although the relative change in each is unknown. A more quantitative analysis has not yet been performed. It can be speculated that the dislocation-related energy level remains constant with respect to the vacuum level, while the conduction band edge moves upward.

The thick layer InAs samples (Nos. 6–9 in Table II) display a thickness dependence of the sheet carrier concentration. The N_s versus t plot is linear with a zero thickness intercept of 9.0×10^{12} cm^{-2}, as seen in Fig. 8. The linearity is indicative of a constant bulk carrier concentration ($\sim5\times10^{16}$ cm^{-3}) from the InAs epilayer, in addition to the constant N_s contribution from the interface. These bulk carriers could be generated by states associated with threading dislocations. The comparative values at 77 K indicates that the bulk carriers in InAs are subject to a partial freeze out. There are thus two parallel channels or pathways for conduction:[4] (i) a high carrier concentration, low mobility interface channel, and (ii) a lower carrier density, high mobility bulk channel. As thickness is increased, the contribution of the bulk channel increases, as evidenced by the sharp rise in mobility. Using this two channel model Chen[4] has calculated that the electron mobility in the InAs epilayer (bulk channel) exceeds 20 000 $cm^2/V\,s$ at 77 K—nearly 2/3 the theoretical electron mobility of InAs (33 000 $cm^2/V\,s$).

The dense TD network ($\sim10^{10}$ cm^{-2}) in the epilayer thus does not appear to scatter carriers strongly. This is in contrast to the strong scattering exhibited by the MD network. The InAs/GaP system is promising for high speed device applications despite having a high defect density.

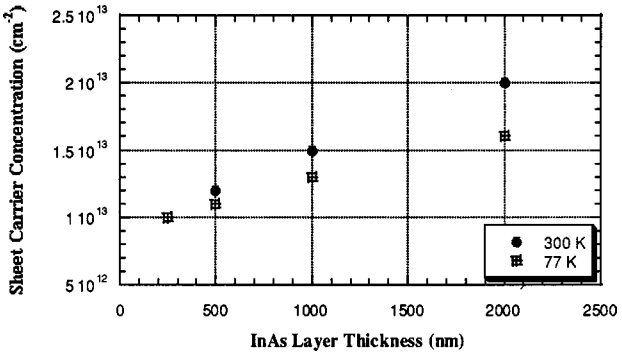

FIG. 8. Dependence of sheet carrier concentration on epilayer thickness for the thick InAs layer samples.

IV. CONCLUSIONS

We have investigated the evolution of the dislocation microstructure during the MBE growth of InAs on GaP and the electronic behavior of the defects. MD introduction occurs by two distinct mechanisms and the resulting microstructure consists mainly of 90° edge MDs, but also a few closely spaced pairs of 60° dislocations. We have demonstrated the existence of a dense sheet of electron charge at the heterointerface, which is linked to the MD network. A defect structure proposed to occur at the intersection of 90° MDs is a likely source of the carriers and may act as an ordered structural dopant. Two parallel conducting pathways for lateral carrier transport in InAs epilayers were proposed—a low mobility interface pathway and a high mobility bulk pathway. High mobility in the bulk channel is achieved despite a high density of TDs.

ACKNOWLEDGMENTS

The authors thank Dr. A. L. Vasiliev for assistance in TEM. This research was funded by the National Science Foundation through Grant No. 9400415-DMR.

[1]E. P. Kvam and S. B. Samavedam, J. Minerals, Metals, Mater. Soc. **46**, 47 (1994).
[2]A. E. Romanov, W. Pompe, S. Mathis, G. E. Beltz, and J. S. Speck, J. Appl. Phys. **85**, 182 (1999).
[3]J. C. P. Chang, T. P. Chin, and J. M. Woodall, Appl. Phys. Lett. **69**, 981 (1996).
[4]E.-H. Chen, Ph.D. thesis, Purdue University, 1998.
[5]J. W. Matthews, S. Mader, and T. B. Light, J. Appl. Phys. **41**, 3800 (1970).

[6]E. P. Kvam, D. M. Maher, and C. J. Humphreys, J. Mater. Res. **5**, 1900 (1990).
[7]F. K. LeGoues, J. Tersoff, M. C. Reuter, M. Hammar, and R. Tromp, Appl. Phys. Lett. **67**, 2317 (1995).
[8]M. Mostoller, M. F. Chisholm, and T. Kaplan, Phys. Rev. Lett. **72**, 1494 (1994).
[9]V. Gopal, E. P. Kvam, T. P. Chin, and J. M. Woodall, Appl. Phys. Lett. **72**, 2319 (1998).